

2-22-1996

New Model for Electron-Impact Ionization Cross Sections of Molecules

W. Hwang

National Institute of Standards and Technology, Gaithersburg, Maryland 20899

Y.-K. Kim

National Institute of Standards and Technology, Gaithersburg, Maryland 20899

M. Eugene Rudd

University of Nebraska - Lincoln, erudd@unl.edu

Follow this and additional works at: <http://digitalcommons.unl.edu/physicsrudd>



Part of the [Physics Commons](#)

Hwang, W.; Kim, Y.-K.; and Rudd, M. Eugene, "New Model for Electron-Impact Ionization Cross Sections of Molecules" (1996). *M. Eugene Rudd Publications*. Paper 21.

<http://digitalcommons.unl.edu/physicsrudd/21>

This Article is brought to you for free and open access by the Research Papers in Physics and Astronomy at DigitalCommons@University of Nebraska - Lincoln. It has been accepted for inclusion in M. Eugene Rudd Publications by an authorized administrator of DigitalCommons@University of Nebraska - Lincoln.

New model for electron-impact ionization cross sections of molecules

J. Chem. Phys. 104, 2956 (1996); DOI:10.1063/1.471116

W. Hwang and Y.-K. Kim

National Institute of Standards and Technology, Gaithersburg, Maryland 20899

M. E. Rudd

Department of Physics and Astronomy, University of Nebraska-Lincoln, Lincoln, Nebraska 68588-0111

ABSTRACT

A theoretical model for electron-impact ionization cross sections, which has been developed primarily for atoms and atomic ions, is applied to neutral molecules. The new model combines the binary-encounter theory and the Bethe theory for electron-impact ionization, and uses minimal theoretical data for the ground state of the target molecule, which are readily available from public-domain molecular structure codes such as GAMESS. The theory is called the binary-encounter Bethe (BEB) model, and does not, in principle, involve any adjustable parameters. Applications to 19 molecules, including H₂, NO, CH₂, C₆H₆, and SF₆, are presented, demonstrating that the BEB model provides total ionization cross sections by electron impact from threshold to several keV with an average accuracy of 15% or better at the cross section peak, except for SiF₃. The BEB model can be applied to stable molecules as well as to transient radicals.

History: Received 13 September 1995; accepted 15 November 1995

Permalink: <http://link.aip.org/link/?JCPSA6/104/2956/1>

Keywords: cross sections, electron-, molecule collisions, ground states, ionization, nitrogen oxides, wave functions, hydrogen molecules, impact phenomena

Copyright ©1996 American Institute of Physics.

New model for electron-impact ionization cross sections of molecules

W. Hwang^{a)} and Y.-K. Kim

National Institute of Standards and Technology, Gaithersburg, Maryland 20899

M. E. Rudd

Department of Physics and Astronomy, University of Nebraska-Lincoln, Lincoln, Nebraska 68588-0111

(Received 13 September 1995; accepted 15 November 1995)

A theoretical model for electron-impact ionization cross sections, which has been developed primarily for atoms and atomic ions, is applied to neutral molecules. The new model combines the binary-encounter theory and the Bethe theory for electron-impact ionization, and uses minimal theoretical data for the ground state of the target molecule, which are readily available from public-domain molecular structure codes such as GAMESS. The theory is called the binary-encounter Bethe (BEB) model, and does not, in principle, involve any adjustable parameters. Applications to 19 molecules, including H₂, NO, CH₂, C₆H₆, and SF₆, are presented, demonstrating that the BEB model provides total ionization cross sections by electron impact from threshold to several keV with an average accuracy of 15% or better at the cross section peak, except for SiF₃. The BEB model can be applied to stable molecules as well as to transient radicals. © 1996 American Institute of Physics. [S0021-9606(96)01708-X]

I. INTRODUCTION

Although there are several useful theories for electron-impact ionization cross sections for atoms and atomic ions, few of them are extendable to neutral molecules and molecular ions, primarily because it is difficult to calculate molecular continuum wave functions, which most of these theories require. In addition, the collision of slow incident electrons with a target requires an approach that treats the incident electron and the bound electrons in the target (or at least the electron being ejected) on equal footing as a compound system, for instance, by introducing strong coupling and exchange interaction between them. This is one of the major reasons for the failure of most theories, particularly those based on the perturbation approach, at low incident electron energies. At high incident electron energies, the plane-wave Born approximation provides accurate ionization cross sections when used with reliable initial- and final-state wave functions.

Strong coupling theories which treat the colliding system as a compound system, such as the close-coupling or the *R*-matrix method, require a large basis set to describe the system, making it very difficult to treat ionizing collisions. Moreover, strong coupling theories tend to produce a large number of resonances, both real and virtual, which may have to be averaged over for practical applications, such as in the modeling of plasma chemistry and radiation effects. Except for a very recent theoretical method called the convergent close-coupling method,¹ these strong coupling theories are mostly limited to discrete excitations and difficult to extend to ionization.

In this article, we describe a new theoretical method that provides reliable electron-impact ionization cross sections for molecules using very simple input data, all of which can

be obtained from standard molecular wave function codes for the ground state of a molecule. There are no adjustable or fitted parameters in our theory. Our method does not provide details of resonances in the continuum, vibrational and/or rotational excitations concomitant with ionization, multiple ionization, dissociative ionization, etc. It simply predicts the total ionization cross section as the sum of ionization cross sections for ejecting one electron from each of the atomic or molecular orbital. We will show that it is valid over the entire energy range, from the first ionization threshold up to several keV in incident electron energies.

As is outlined in Sec. II, our theory combines the Mott cross section² modified by the binary-encounter theory³ for low incident energies *T* with the Bethe theory⁴ for high *T*. Many models have been proposed to use this combination,⁵⁻⁸ but they all require either some empirical parameters or explicit knowledge of the continuum dipole oscillator strengths of the target molecule or its constituent atoms. Some of these models require empirical parameters which are difficult to obtain, or use a large number of such parameters. Our model uses a new way to determine the ratio between the low-*T* and high-*T* cross sections without using any empirical parameters, and ionization cross sections are derived from analytic expressions for the entire range of *T* with three molecular constants per molecular orbital, which are available from molecular structure codes. Deep inner shells do not contribute appreciably to total ionization cross sections; hence they can be omitted in most theories for total ionization cross sections including ours.

Because of its simplicity, our theory can predict cross sections for complex molecules such as C₃H₈ and SF₆ as easily as for simple ones such as H₂. Moreover, our theory can be applied not only to stable molecules but also to transient radicals. The applicability of our theory is limited only by the availability of a molecular structure code that can provide basic information on molecular orbitals. Judging

^{a)}Present address: Ultraprecision Technology Team, Samsung Electronics Co., Suwon, Korea.

from the examples presented in this article and our experience with other atoms and molecules, our theory can provide total ionization cross sections accurate enough to be used in modeling of plasma chemistry, magnetic fusion plasmas, and radiation effects.

Two other theoretical methods to estimate ionization cross sections with comparable flexibility are the “DM approach” based on an additivity rule developed by Deutsch *et al.*⁶ and the Weizsäcker–Williams method (“WW method”) as modified by Seltzer.⁸ The DM approach constructs a molecular ionization cross section by adding ionization cross sections for the constituent atoms. The basic shape of these atomic cross sections is given by the classical theory of Gryzinski,⁹ while their absolute values are given in terms of (a) atomic orbital radii, which can be obtained from atomic wave function codes, (b) atomic orbital occupation numbers, which are derived from the Mulliken population analysis of the target molecule, and (c) atomic weighting factors, which have been fitted to known atomic ionization cross sections. Our theory uses far fewer, *ab initio* molecular parameters which are also standard output of molecular structure codes. Although the BEB model does not require any experimental data since theoretical values of binding energy B and kinetic energy U are available, we prefer to use the experimental value for the ionization potential of the outermost electron to obtain the correct threshold for comparison to experiments. The threshold behavior of ionization cross sections is sensitive to the value of the lowest *electron* binding energy (not the dissociation energy!). The WW method⁸ is very similar to our BED model described in the next section in that it requires explicit data on continuum dipole oscillator strengths of the target. However, the WW method is primarily designed for high-energy incident electrons, and may lead to unrealistic results for slow incident electrons of hundreds of eV or lower.

The underlying theory of our model is outlined in Sec. II, application examples are described in Sec. III, and conclusions are presented in Sec. IV.

II. OUTLINE OF THEORY

Recently, we proposed the binary-encounter-dipole (BED) model for electron-impact ionization cross sections of atoms and molecules.¹⁰ This BED model combines the binary-encounter theory³ and the Bethe theory.⁴ The ratio between the binary-encounter theory and the Bethe theory is set by requiring the asymptotic form at high incident energy T of the former to match that of the latter both in the ionization cross section and in the stopping cross section. The stopping cross section, which is the integral of the product of the energy-loss cross section and the energy loss of the incident electron, is used to evaluate the stopping power of the target medium. The BED model provides a formula to calculate the singly differential cross section, or the energy distribution of ejected electrons $d\sigma/dW$ with the ejected electron energy W , for each atomic or molecular orbital. To apply the BED model, one needs for each orbital the electron binding energy B , the average kinetic energy $U = \langle \mathbf{p}^2/2m \rangle$ with the bound

electron momentum \mathbf{p} and its mass m , the orbital occupation number N and the continuum dipole oscillator strength df/dW .

The value of the kinetic energy U for each orbital in the initial state (usually the ground state) of the target is a theoretical quantity evaluated in any atomic or molecular wave function code that calculates the total energy. However, both the initial- and continuum-state wave functions are needed to calculate df/dW and this is the only nontrivial data needed to apply the BED model. Alternatively, df/dW can be deduced from experimental photoionization cross sections, though partial cross sections are needed to deduce df/dW for each orbital. The total ionization cross section σ_i is then obtained by integrating $d\sigma/dW$ over the allowed range of W , i.e., from 0 to $(T-B)/2$

$$\sigma_i(t) = \frac{S}{t+u+1} \left[D(t) \ln t + \left(2 - \frac{N_i}{N} \right) \left(\frac{t-1}{t} - \frac{\ln t}{t+1} \right) \right], \quad (1)$$

where $t = T/B$, $u = U/B$, $S = 4\pi a_0^2 N R^2/B^2$, $a_0 = 0.5292 \text{ \AA}$, $R = 13.61 \text{ eV}$,

$$D(t) \equiv N^{-1} \int_0^{(t-1)/2} \frac{1}{w+1} \frac{df(w)}{dw} dw, \quad (2)$$

with $w = W/B$, and

$$N_i \equiv \int_0^\infty \frac{df(w)}{dw} dw. \quad (3)$$

The BED model was found to be very effective in reproducing known values of $d\sigma/dW$ and σ_i for small atoms and molecules, demonstrating an agreement of $\pm 10\%$ or better for the entire range of incident electron energies in most cases.¹⁰

Although one can in principle calculate df/dW for each orbital, it is available only for a limited number of atoms and very few molecules. Hence, we also proposed a simplified version of the BED theory when no information on df/dW is available. In this case, which we refer to as the binary-encounter-Bethe (BEB) model,¹⁰ we assume a simple form for df/dW ,

$$\frac{df}{dw} = N/(w+1)^2 \quad (4)$$

such that the integrated cross section σ_{BEB} per orbital is given by

$$\sigma_{\text{BEB}} = \frac{S}{t+u+1} \left[\frac{\ln t}{2} \left(1 - \frac{1}{t^2} \right) + 1 - \frac{1}{t} - \frac{\ln t}{t+1} \right]. \quad (5)$$

Equation (4) approximates the shape of df/dW for the ionization of the ground state of H and generates reliable differential ionization cross sections only for the targets with simple shell structures,¹⁰ such as H, He, and H₂.

In Eqs. (1) and (5), the term associated with the first logarithmic function on the right-hand side (RHS) represents distant collisions (large impact parameters) dominated by the dipole interaction, and the rest of the terms on the RHS represent close collisions (small impact parameters) as described by the Mott cross section. The second logarithmic

TABLE I. Molecular orbitals, electron binding energy B in eV, kinetic energy U in eV, and electron occupation number N for H_2 , N_2 , O_2 , CO , NO , H_2O , CO_2 , and NH_3 . All B and U values are theoretical, except for those marked by an asterisk, which are experimental.

Molecule	MO	B	U	N
H_2	$1\sigma_g$	15.43*	15.98	2
N_2	$2\sigma_g$	41.72	71.13	2
	$2\sigma_u$	21.00	63.18	2
	$1\pi_u$	17.07	44.30	4
	$3\sigma_g$	15.58*	54.91	2
O_2 , triplet	$2\sigma_g$	46.19	79.73	2
	Average of α and β orbital values	$2\sigma_u$	29.82	90.92
Average of α and β orbital values	$1\pi_u$	19.64	59.89	4
	$3\sigma_g$	19.79	71.84	2
	$1\pi_g$	12.07*	84.88	2
	CO	3σ	41.92	79.63
4σ		21.92	73.18	2
1π		17.66	54.30	4
5σ		14.01*	42.26	2
NO , doublet	3σ	43.70	76.55	2
	Average of α and β orbital values	4σ	25.32	77.04
Average of α and β orbital values	1π	18.49	55.37	4
	5σ	15.87*	62.25	2
	2π	9.26*	65.27	1
	H_2O	$2a_1$	36.88	70.71
$1b_2$		19.83	48.36	2
$3a_1$		15.57	59.52	2
$1b_1$		12.61*	61.91	2
CO_2	$3\sigma_{1g}$	42.04	75.72	2
	$2\sigma_{2u}$	40.60	78.38	2
	$4\sigma_{1g}$	21.62	74.66	2
	$3\sigma_{2u}$	20.27	71.56	2
	$1\pi_u$	19.70	49.97	4
	$1\pi_g$	13.77*	64.43	4
NH_3	$2a_1$	31.13	48.49	2
	$1e$	17.19	35.62	4
	$3a_1$	10.16*	43.25	2

function originates from the interference of the direct and exchange scattering also described by the Mott cross section.

We present the values of B , U , and N for small molecules in Table I, those for hydrocarbons in Table II, and the data for SiF_x , $x=1-3$, and SF_6 in Table III. The data for H_2 are from the correlated wavefunction of Kotos and Roothaan,¹¹ while the rest of the data in Tables I–III are from the molecular structure code GAMESS.¹² Since deep inner shells, such as the K shells of N_2 and O_2 , contribute little to total ionization cross sections, we have omitted them from the tables, though we included them to calculate BEB cross sections for small molecules.

One can use either theoretical or experimental values of B , while U is a theoretical quantity that cannot be directly measured, though the sum of all U 's is equal to the total energy of the target molecule according to the virial theorem. Since experimental values of B are often smaller than theoretical ones, the BEB cross sections obtained using experimental B values are usually higher (by 10%–15% at the

TABLE II. Molecular orbitals, electron binding energy B in eV, kinetic energy U in eV, and electron occupation number N for hydrocarbons. All B and U values are theoretical, except for those marked by an asterisk, which are experimental.

Molecule	MO	B	U	N	
CH_2 , triplet	$2a_1$	23.59	35.20	2	
	Average of α and β orbital values	$1b_1$	16.43	26.70	2
	$3a_1$	12.32	31.88	1	
Average of α and β orbital values	$1b_2$	10.40*	31.80	1	
	CH_3 , doublet	$2a_1$	24.57	34.18	2
		Average of α and β orbital values	$1e$	15.64	26.46
Average of α and β orbital values	$3a_1$	9.84*	30.40	1	
	CH_4	$2a_1$	25.73	33.05	2
$1t_2$		12.51*	25.96	6	
C_2H_4	$2a_g$	28.23	40.97	2	
	$2b_{2u}$	21.56	33.49	2	
	$1b_{3u}$	17.55	25.33	2	
	$3a_g$	16.08	35.00	2	
	$1b_{1g}$	13.74	28.56	2	
C_2H_6	$1b_{1u}$	10.51*	26.51	2	
	$2a_{1g}$	27.75	34.37	2	
	$2a_{2u}$	22.99	33.60	2	
	$1e_u$	16.31	24.42	4	
	$3a_{1g}$	13.90	32.78	2	
C_3H_8	$1e_g$	11.52*	28.17	4	
	$3a_1$	28.69	34.45	2	
	$2b_1$	25.25	34.96	2	
	$4a_1$	21.86	33.32	2	
	$1b_2$	17.04	23.46	2	
	$5a_1$	16.30	25.80	2	
	$3b_1$	15.03	28.08	2	
	$1a_2$	14.53	27.09	2	
	$6a_1$	12.98	31.21	2	
	$4b_1$	12.97	34.09	2	
$2b_2$	10.95*	28.53	2		
C_6H_6	$2a_{1g}$	31.38	39.32	2	
	$2e_{1u}$	27.64	42.43	4	
	$2e_{2g}$	22.42	39.00	4	
	$3a_{1g}$	19.38	25.38	2	
	$2b_{1u}$	17.50	34.21	2	
	$1b_{2u}$	16.86	40.02	2	
	$3e_{1u}$	16.03	32.58	4	
	$1a_{2u}$	13.67	23.90	2	
	$3e_{2g}$	13.45	37.96	4	
$1e_{1g}$	9.25*	28.27	4		

cross section peak) than those obtained using theoretical B values. Using the experimental value for the lowest electron binding energy (=first ionization potential) will not only assure that the cross section starts at the right threshold but also we found that the shape and magnitude of the BEB cross section near the threshold agree better with known experimental cross sections. On the other hand, the cross sections with theoretical values of B tend to agree better with experiment near the peak ($T \sim 100$ eV).

For closed-shell molecules, we used the restricted Hartree–Fock (RHF) method with the default Gaussian basis set (known as the 6-311-G set) provided by the GAMESS code. For open-shell molecules, we found that the unre-

TABLE III. Molecular orbitals, electron binding energy B in eV, kinetic energy U in eV, and electron occupation number N for SiF_x , $x=1-3$, and SF_6 . All B and U values are theoretical, except for those marked by an asterisk, which are experimental. Atomic orbitals which contribute $\geq 90\%$ of molecular charge density are identified in parentheses.

Molecule	MO	B	U	N
SiF, quartet average of α and β orbital values	3σ (Si $2s$)	168.63	359.53	2
	1π (Si $2p$)	117.15	332.44	4
	4σ (Si $2p$)	117.18	331.55	2
	5σ	42.84	104.41	2
	6σ	19.99	74.82	2
	2π	17.84	81.34	4
	7σ (Si $3s$)	16.30	55.09/3	1
	3π (Si $3p$)	7.28*	34.39/3	2
SiF ₂	$3a_1$ (Si $2s$)	169.13	360.19	2
	$2b_1$ (Si $2p$)	117.52	331.76	2
	$4a_1$ (Si $2p$)	117.47	332.52	2
	$1b_2$ (Si $2p$)	117.47	331.38	2
	$5a_1$ (F $2s$)	43.89	102.17	2
	$3b_1$ (F $2s$)	43.22	106.55	2
	$6a_1$	21.56	80.10	2
	$4b_1$	19.53	84.66	2
	$7a_1$	18.97	77.67	2
	$2b_2$	18.60	77.19	2
	$1a_2$ (F $2p$)	17.75	83.62	2
	$5b_1$ (F $2p$)	17.36	88.13	2
$8a_1$ (Si $3s$)	10.78*	46.19/3	2	
SiF ₃ , doublet average of α and β orbital values	$3a_1$ (Si $2s$)	170.32	359.73	2
	$4a_1$ (Si $2p$)	118.79	332.26	2
	$2e$ (Si $2p$)	118.85	331.83	4
	$5a_1$	44.75	101.00	2
	$3e$	43.95	106.28	4
	$6a_1$	22.57	81.11	2
	$4e$	20.47	82.42	4
	$7a_1$	19.71	75.76	2
	$5e$	19.03	82.66	4
	$6e$ (F)	18.29	85.84	4
	$1a_2$ (F)	17.86	88.76	2
	$8a_1$ (Si $3s$)	9.3*	52.38/3	1
SF ₆	$3a_{1g}$ (S $2s$)	256.18	510.35	2
	$2t_{1u}$ (S $2p$)	193.27	479.25	6
	$4a_{1g}$	50.93	85.62	2
	$3t_{1u}$	47.09	101.6	6
	$2e_g$	45.50	110.3	4
	$5a_{1g}$	30.32	98.55	2
	$4t_{1u}$	25.61	83.20	6
	$1t_{2g}$	23.03	75.55	6
	$3e_g$	20.35	86.84	4
	$1t_{2u}$ (F)	20.06	90.74	6
	$5t_{1u}$	19.69	91.23	6
	$1t_{1g}$ (F)	15.33*	98.29	6

stricted Hartree–Fock (UHF) method produced more realistic orbital energies—which we took as the electron binding energies as prescribed by the Koopman theorem—for valence orbitals than the restricted open-shell Hartree–Fock (ROHF) method. Although the UHF method has the disadvantage of producing “too many” orbital and kinetic energies— α and β orbitals—the valence orbital energies from the ROHF method were often unrealistically small, making the corresponding cross section too large, sometimes by as much as 50% at the cross section peak. On the other

hand, using B and U values from the UHF method produces cross sections almost identical to those produced using the average between the B and U values from the matching α and β orbitals. The B and U values presented in Tables I–III are these average values for open-shell molecules.

Deducing experimental B values for inner orbitals is not straightforward for molecules, particularly when the outermost orbital is only partially occupied, in addition to the ambiguity of whether to use the “vertical” or “relaxed” binding energies. In practice, the BEB model is insensitive to minor variations in the values of B and U used, except for the lowest B . For these reasons, we have used the experimental values for the lowest B , which are available for many molecules and radicals,¹³ and theoretical values for the remaining orbitals.

Most B values listed in Tables I–III are slightly different from those quoted in Rudd *et al.*¹⁴ because the experimental B values were quoted in the latter, while we used mostly theoretical values in the present work. Also, some U values in Ref. 14—e.g., for NH_3 , H_2O —are too high because they were not divided by the electron occupation numbers, or in some cases—e.g., for SF_6 and TeF_6 —too low because pseudopotentials were used. The inner-shell molecular orbitals from pseudopotentials lack nodes in the core region, leading to unrealistically low U values. Minor differences in the U values resulted also from the use of different molecular wave function codes in the present work and Ref. 14. We recommend the values in Tables I–III.

III. APPLICATIONS TO MOLECULES

In this section, we compare our theoretical cross sections, mostly BEB but some BED cross sections, to a large number of molecules. Most older experiments measured the “gross” ionization cross section, which is determined by measuring the total ion current rather than the number of ions. On the other hand, most theoretical values are the “counting” ionization cross section, which accounts for the number of ions produced. When many multiply charged ions are produced, the gross ionization cross section will be significantly larger than the counting ionization cross section. The cross sections based on the BEB and BED models are counting ionization cross sections, and therefore should be considered as the lower limits to experimental gross ionization cross sections. In modern experiments, both molecular ions as well as their fragments are often collected using mass spectrometers. Since the BEB and BED cross sections are simple sums of cross sections for ejecting one electron from each molecular orbital, the theory cannot give a detailed account of dissociative ionization or fragments produced. Hence, comparisons of the theory with experiments on large molecules with diverse channels for dissociative ionization and fragmentation are not straightforward. For simplicity, we compared our theoretical cross sections to the simple sum of all experimental partial cross sections that produced an ion. Nevertheless, the comparisons presented here will clearly demonstrate the utility of our theory, which is applicable to a wide range of molecules.

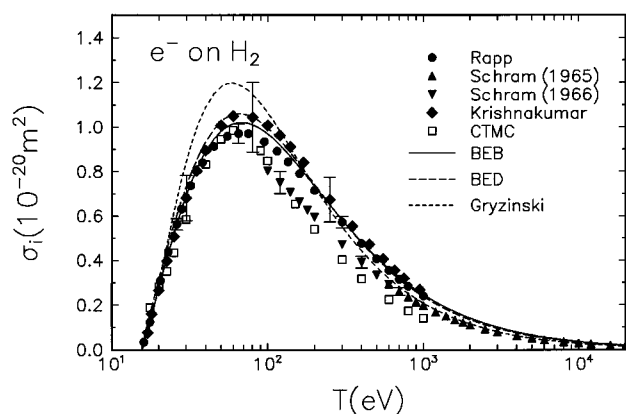


FIG. 1. Comparison of the BED and BEB cross sections to other theory and experiment for H_2 . Solid curve, the BEB cross section; long-dashed curve, the BED cross section (Ref. 10); short-dashed curve, classical theory (Ref. 9); squares, CTMC theory (Ref. 19); circles, experimental data by Rapp and Englander-Golden (Ref. 15); triangles, data by Schram *et al.* (Ref. 17); inverted triangles, Schram *et al.* (Ref. 18); diamonds, data by Krishnakumar and Srivastava (Ref. 16).

A. Diatomic molecules

In Fig. 1, we compare our BEB cross section for H_2 to the experimental data by Rapp and Englander-Golden,¹⁵ the data by Krishnakumar and Srivastava,¹⁶ those by Schram *et al.*,^{17,18} the BED cross section in which accurate experimental df/dW was used,¹⁰ classical cross section by Gryzinski,⁹ and the classical trajectory Monte Carlo (CTMC) cross section by Schultz *et al.*¹⁹ The BED cross section in Fig. 1 is slightly higher than that shown in Fig. 7 of Ref. 10 because the U value used there was wrong. The correct value is given in Table I. The classical theory of Gryzinski⁹ tends to overestimate the peak value not only of H_2 but also of other targets, such as H and N_2 .^{10,20}

Although the BEB model seems to agree slightly better with the cross section by Rapp and Englander-Golden than the BED model at the peak, the latter will definitely provide better differential cross sections, particularly for more complex targets where electron correlation strongly affects the df/dW of valence shells. The high accuracy ($\pm 4.5\%$) claimed by Rapp and Englander-Golden implies that the excellent agreement between the BED cross section and the data by Krishnakumar and Srivastava near the cross section peak is accidental. The CTMC cross section at high T falls short of experimental values because the CTMC theory lacks the dipole contribution, which dominates at high T . The experimental data by Schram *et al.* are too low despite the high accuracy ($\pm 6.7\%$) claimed by the authors.

Existing experimental photoionization data of N_2 were analyzed earlier¹⁴ and the df/dW for outer molecular orbitals are available. These data were used to derive the BED cross section, Eq. (1), for N_2 . The BED and BEB cross sections for N_2 are compared in Fig. 2 to the experimental data by Rapp and Englander-Golden,¹⁵ the data by Schram *et al.*,^{17,18} the data by Krishnakumar and Srivastava,²¹ and very recent experimental data by Straub *et al.*²² The experimental uncer-

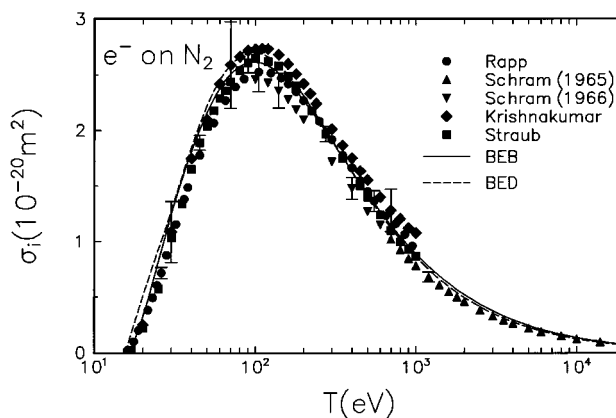


FIG. 2. Comparison of the BED and BEB cross sections to experiment for N_2 . Solid curve, the BEB cross section; dashed curve, the BED cross section; circles, experimental data by Rapp and Englander-Golden (Ref. 15); triangles, data by Schram *et al.* (Ref. 17); inverted triangles, data by Schram *et al.* (Ref. 18); diamonds, Krishnakumar and Srivastava (Ref. 21); squares, data by Straub *et al.* (Ref. 22).

tainty of the data by Straub *et al.*, $\pm 3.5\%$, is the smallest among the data cited in this article, while the uncertainty of the data by Rapp and Englander-Golden is $\pm 7\%$, and that of the data by Krishnakumar and Srivastava is $\pm 15\%$. As in the case of H_2 , the BEB cross section agrees with the experiments better than the BED cross section in the vicinity of the threshold. However, since the BED model uses the actual continuum dipole oscillator strengths, its high- T behavior and the energy distribution of ejected electrons should be more reliable than those of the BEB model. Note that the data by Straub *et al.* are in excellent agreement with the BED cross section for $T \geq 300$ eV, while the data by Rapp and Englander-Golden for $T > 500$ eV are slightly higher, a general trend also seen in their cross sections for other targets.

In Fig. 3, the BEB cross section for O_2 is compared to the experimental data by Rapp and Englander-Golden,¹⁵ the

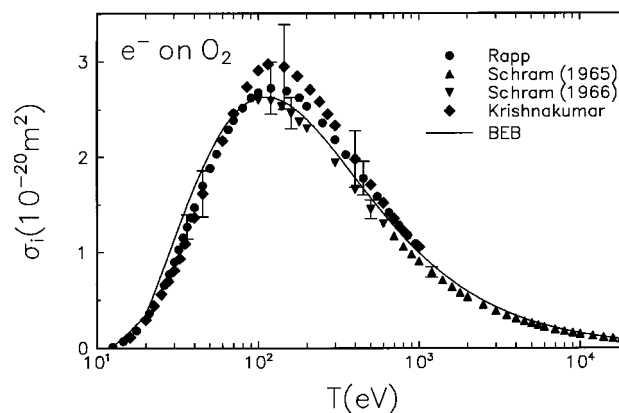


FIG. 3. Comparison of the BEB cross section to experiment for O_2 . Solid curve, the BEB cross section; circles, experimental data by Rapp and Englander-Golden (Ref. 15); triangles, data by Schram *et al.* (Ref. 17); inverted triangles, data by Schram *et al.* (Ref. 18); diamonds, data by Krishnakumar and Srivastava (Ref. 23).

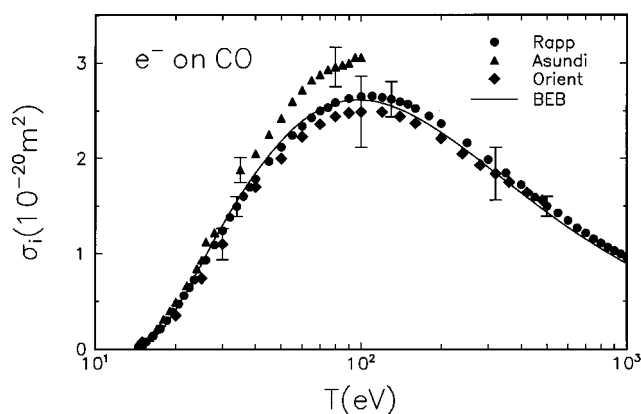


FIG. 4. Comparison of the BEB cross section to experiment for CO. Solid curve, the BEB cross section; circles, experimental data by Rapp and Englander-Golden (Ref. 15); triangles, data by Asundi *et al.* (Ref. 24); diamonds, data by Orient and Srivastava (Ref. 25).

data by Schram *et al.*,^{17,18} and those by Krishnakumar and Srivastava.²³ Unlike the case of H₂ and N₂, the BEB cross section is lower near the peak than the experimental values by Rapp and Englander-Golden. This is the first case in which we used the UHF method for the wave function and took the average of the α and β orbital values. The theoretical B values for the outer valence orbitals did not agree well with known experimental values, which we interpret as an indication that a better wave function may be needed.

In Fig. 4, the BEB cross section for CO is compared to the experimental data by Rapp and Englander-Golden,¹⁵ the data by Asundi *et al.*,²⁴ and those by Orient and Srivastava.²⁵ The data by Asundi *et al.* seem to be in clear disagreement not only with other measurements but also with our BEB cross section.

In Fig. 5, the BEB cross section for NO is compared to the experimental data by Rapp and Englander-Golden,¹⁵ and those by Iga *et al.*²⁶ The B values of NO require special attention because there are many ionization potentials corre-

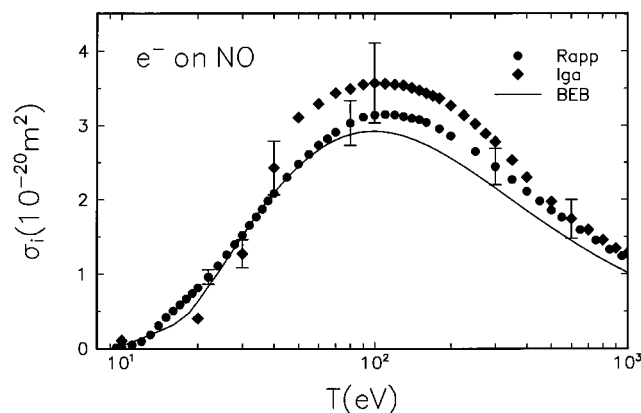


FIG. 5. Comparison of the BEB cross section to experiment for NO. Solid curve, the BEB cross section; circles, experimental data by Rapp and Englander-Golden (Ref. 15); diamonds, data by Iga *et al.* (Ref. 26).

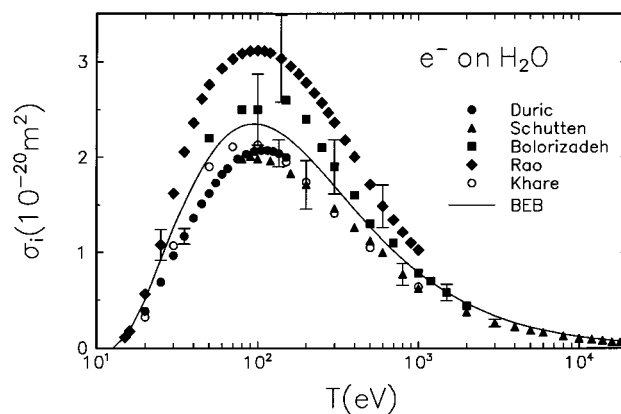


FIG. 6. Comparison of the BEB cross section to experiment for H₂O. Solid curve, the BEB cross section; open circles, semiempirical theory by Khare and Meath (Ref. 5); filled circles, experimental data by Durić *et al.* (Ref. 29); triangles, data by Schutten *et al.* (Ref. 31); squares, data by Bolorizadeh and Rudd (Ref. 30); diamonds, data by Rao *et al.* (Ref. 32).

sponding to many ionic states generated by the ionization of a 5σ or 1π electron. Among these ionic states, the $^3\Pi$ state created by the ionization of a 5σ electron dominates the photoionization cross section measured using a photon of ~ 21 eV in energy.²⁷ Although we do not expect the electron-impact ionization cross sections to have the same ratios as those by photoionization, we assumed that the threshold behavior would be similar, and used the experimental values of B for the 5σ orbital and the 2π orbital in the BEB cross section shown in Fig. 5. The average value of the theoretical orbital energies for the 5σ orbital is 18.55 eV. The “kink” near $T=20$ eV is the artifact of the BEB model because the model cannot account for autoionizing states between the lowest B and $T\sim 20$ eV that must have been included in the experimental cross sections. Indeed, the experimental data by Kim *et al.*²⁸ (not shown in the figure) agree very well with those by Rapp and Englander-Golden for $T\leq 40$ eV, indicating that the experimental data by Iga *et al.* at $10 < T < 30$ eV are too low.

B. H₂O, CO₂, and NH₃

In Fig. 6, the BEB cross section for H₂O is compared to the experimental data by Durić *et al.*,²⁹ the data by Bolorizadeh and Rudd,³⁰ the data by Schutten *et al.*,³¹ and the data by Rao *et al.*³² The performance of the BEB cross sections observed in closed-shell diatomic molecules indicates that the peak values of the data by Rao *et al.* are likely to be too high, and those by Schutten *et al.* too low. The theoretical cross section by Khare and Meath,⁵ which uses experimental df/dW and other fitted parameters, is lower than our cross section, but the difference is within the uncertainty of our model, about $\pm 15\%$, at the cross section peak.

The BEB cross section for CO₂ shown in Fig. 7 agrees better with the experimental data by Rapp and Englander-Golden¹⁵ than the data by Orient and Srivastava²⁵ near the peak, though the BEB peak value is within the uncertainty of the data by Orient and Srivastava. The shape of

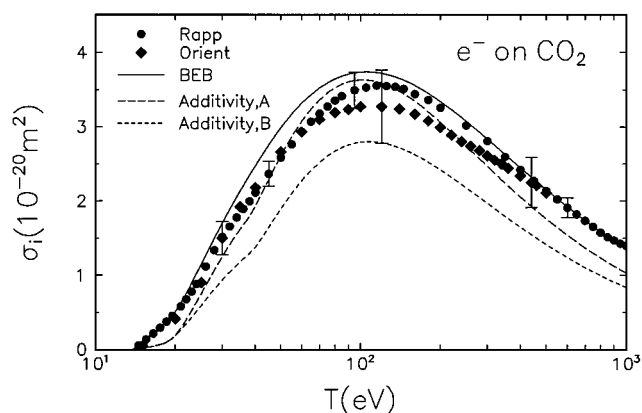


FIG. 7. Comparison of the BEB cross section to experiment for CO_2 . Solid curve, the BEB cross section; long-dashed curve, semiempirical additivity rule with 32 constants (Ref. 20); short-dashed curve, semiempirical additivity rule with 60 constants (Ref. 20); circles, experimental data by Rapp and Englander-Golden (Ref. 15); triangles, data by Orient and Srivastava (Ref. 25).

the cross section by Orient and Srivastava at $T > 200$ eV suggests that their values are decreasing too slowly, indicating a systematic trend. One of the two semiclassical cross sections by Margreiter *et al.*²⁰ (marked A in Fig. 7) based on the DM approach, which is an additivity rule discussed in Sec. I, agrees well with experiments except at the very highest incident energies.

As can be seen from Table I, the BEB cross section used 18 constants for CO_2 , while the DM approach cross sections required 32 constants for curve A and 60 constants for curve B, including 8 and 15 empirical weighting factors, respectively.

As is shown in Fig. 8, the BEB cross section for NH_3 agrees within 10% with the experimental data by Djurić *et al.*³³ and those by Rao and Srivastava³⁴ for $T \geq 40$ eV. No error limits were quoted by Djurić *et al.* As in the case of

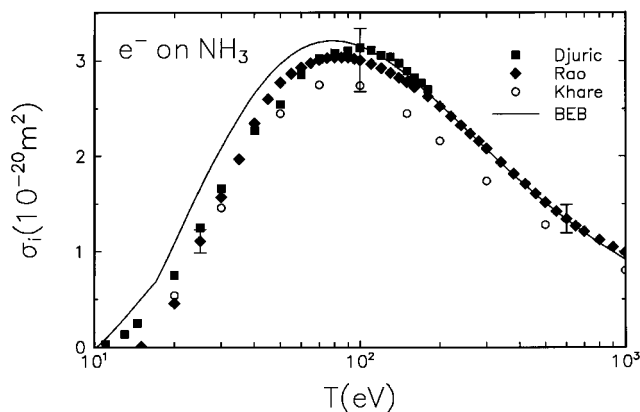


FIG. 8. Comparison of the BEB cross section to experiment for NH_3 . Solid curve, the BEB cross section; circles, semiempirical theory by Khare and Meath (Ref. 5); squares, experimental data by Djurić *et al.* (Ref. 33); diamonds, data by Rao and Srivastava (Ref. 34).

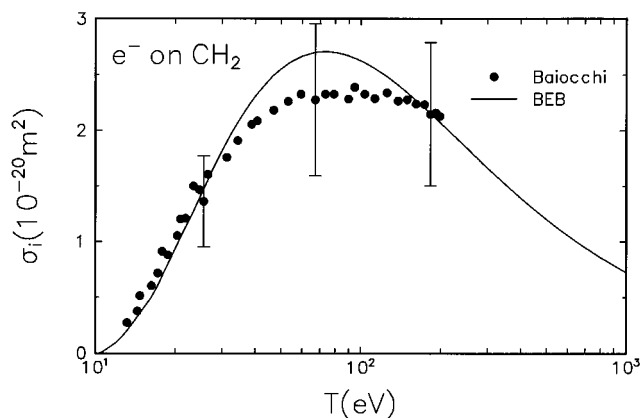


FIG. 9. Comparison of the BEB cross section for CH_2 to experimental data for CD_2 . Solid curve, the BEB cross section; circles, experimental data by Baiocchi *et al.* (Ref. 36).

H_2O , the peak value of the semiempirical cross section by Khare and Meath⁵ is lower than ours, but the difference is within the uncertainty of our model.

C. Hydrocarbons

We found that the BEB model is particularly successful in reproducing known cross sections of hydrocarbons. The DM approach also works well for hydrocarbons.³⁵ The BEB cross sections for CH_2 and CH_3 are compared to the experimental data by Baiocchi *et al.*³⁶ for CD_2 (Fig. 9) and CD_3 (Fig. 10), respectively. The BEB model is not refined enough to account for the isotope substitution. Although the BEB cross sections for these molecules are in good agreement with the experimental data, Fig. 9 indicates that the experimental data for CD_2 are not decreasing as fast as the BEB cross section for $T > 150$ eV. The data by Baiocchi *et al.* is a lower bound to the total ionization cross section because their experiment did not include the cross sections for the production of atomic ions, C^+ and D^+ .

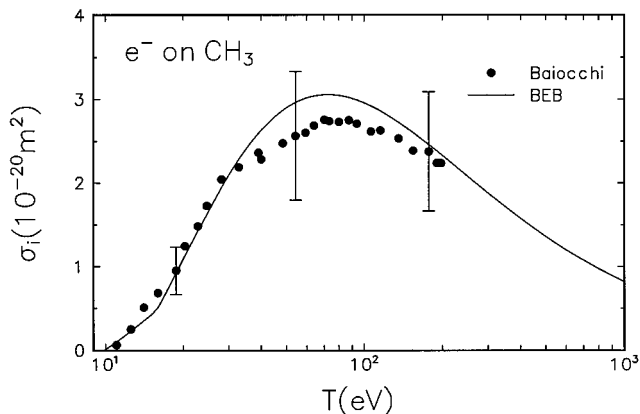


FIG. 10. Comparison of the BEB cross section for CH_3 to experimental data for CD_3 . Solid curve, the BEB cross section; circles, experimental data by Baiocchi *et al.* (Ref. 36).

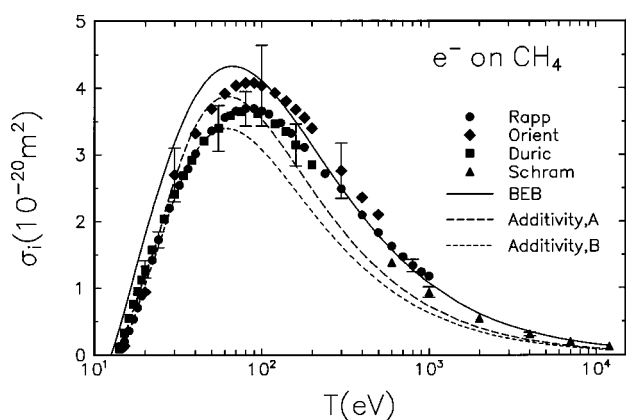


FIG. 11. Comparison of the BEB cross section to experiment for CH_4 . Solid curve, the BEB cross section; long-dashed curve, semiempirical additivity rule with 12 constants (Ref. 20); short-dashed curve, semiempirical additivity rule with 24 constants (Ref. 20); circles, experimental data by Rapp and Englander-Golden (Ref. 15); diamonds, data by Orient and Srivastava (Ref. 25); squares, data by Durić *et al.* (Ref. 38); triangles, data by Schram *et al.* (Ref. 37).

In Fig. 11, the BEB cross section is compared to the experimental data for CH_4 by Rapp and Englander-Golden,¹⁵ the data by Schram *et al.*,³⁷ the data by Orient and Srivastava,²⁵ and the data by Durić *et al.*³⁸ The BEB cross section is too large between the threshold and the peak. We also included the cross sections generated from the additivity rule²⁰ of the DM approach as was done for CO_2 . For methane, the additivity rule uses 12 constants for curve A and 24 constants for curve B. The experimental data by Chatham *et al.*³⁹ (not shown in the figure) are very close to those by Durić *et al.*

The methane molecule has a simple electronic structure (see Table II), and most of its cross section comes from the $1t_2$ valence orbital which has six electrons. The BEB model is vulnerable in this case because any theoretical uncertainty is amplified by the large occupation number of the valence orbital. It may be necessary to use the BED model with reliable continuum dipole oscillator strengths and data from a better molecular wave function to improve the BEB cross section at low T .

In Fig. 12, the BEB cross section is compared to the experimental data for C_2H_4 by Rapp and Englander-Golden,¹⁵ and those by Schram *et al.*³⁷ The BEB cross section and the experimental data by Rapp and Englander-Golden seem to disagree near the peak, but the data by Schram *et al.* are in good agreement with the theory. (Unfortunately, the data by Rapp and Englander-Golden for this molecule stops at $T=145$ eV unlike their data on other targets.)

In Fig. 13, the BEB cross section is compared to the experimental data for C_2H_6 by Durić *et al.*,³⁸ the data by Chatham *et al.*,³⁹ the data by Schram *et al.*,³⁷ and the data by Grill *et al.*⁴⁰ Again, the BEB cross section is in good agreement with the experiments. Unlike the case of smaller molecules, the high- T cross section by Schram *et al.* is now

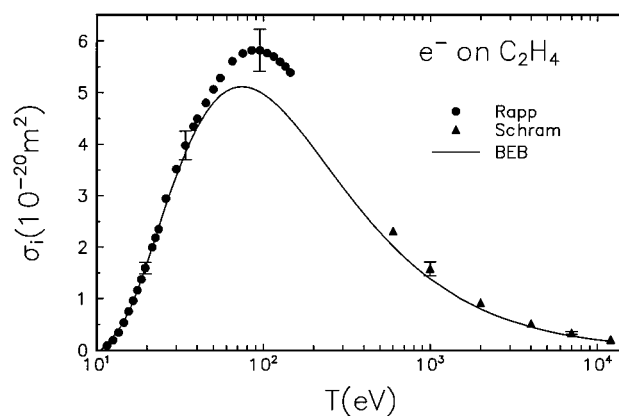


FIG. 12. Comparison of the BEB cross section to experiment for C_2H_4 . Solid curve, the BEB cross section; circles, experimental data by Rapp and Englander-Golden (Ref. 15); triangles, data by Schram *et al.* (Ref. 37).

higher than the BEB cross section. The experimental data by Grill *et al.* agree very well with the BEB cross section at high T , making it likely that the data by Schram *et al.* are too high.

The BEB cross section for C_3H_8 in Fig. 14 is in good agreement with the experimental data by Durić *et al.*³⁸ and by Grill *et al.*⁴¹ but somewhat lower than those by Schram *et al.*³⁷

In Fig. 15, the BEB cross section is compared to the experimental data for C_6H_6 by Schram *et al.*,³⁷ which are available only for $T \geq 600$ eV. Although we expect the BEB cross section to be the lower limit to the gross ionization cross section measured by Schram *et al.*, the discrepancy between theory and experiment seems to be too large. Experimental data at lower T are desirable to determine the reliability of the BEB cross section for large molecules. Unlike the case of methane, there is no single molecular orbital that dominates the ionization cross section of benzene, and hence

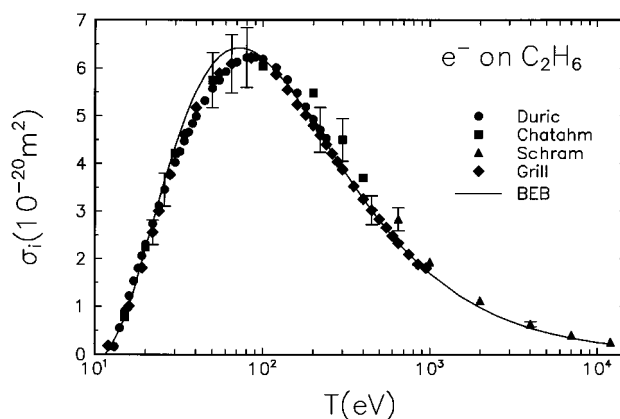


FIG. 13. Comparison of the BEB cross section to experiment for C_2H_6 . Solid curve, the BEB cross section; circles, experimental data by Durić *et al.* (Ref. 38); squares, data by Chatham *et al.* (Ref. 39); triangles, data by Schram *et al.* (Ref. 37); diamonds, data by Grill *et al.* (Ref. 40).

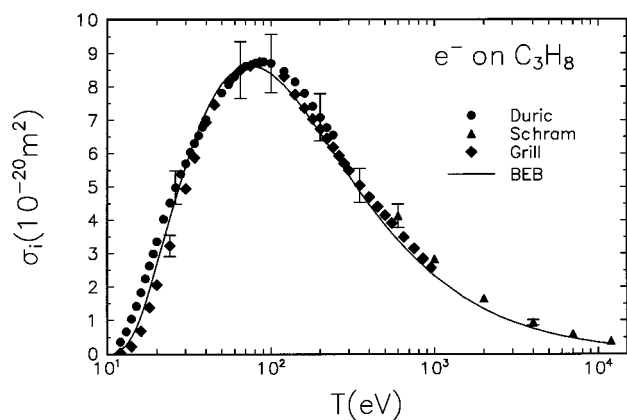


FIG. 14. Comparison of the BEB cross section to experiment for C_3H_8 . Solid curve, the BEB cross section; circles, experimental data by Duric *et al.* (Ref. 38); triangles, data by Schram *et al.* (Ref. 37); diamonds, data by Grill *et al.* (Ref. 41).

we expect the BEB model cross section at low T to be reliable.

D. Fluorine compounds

As was pointed out earlier by Deutsch *et al.*,⁶ fluorine compounds, such as SiF_x , $x = 1-3$, exhibit a peculiar behavior: The ionization cross section for a molecule with more fluorine atoms is smaller than the cross section for a molecule with fewer fluorine atoms.⁴²⁻⁴⁴ This is contrary to the “logic” used in an additivity rule, which expects higher cross sections for molecules with more atoms of the same kind.⁶

The explanation for this “abnormal” behavior is simple; it results from a strong ionic bonding of the F atoms. The four valence electrons in the $3s$ and $3p$ orbitals of Si have much larger orbital radii than those of the $2s$ and $2p$ electrons in F. Hence, the dominant part of the ionization cross section comes from the valence electrons of Si. When one F atom is combined to form SiF, only one valence electron

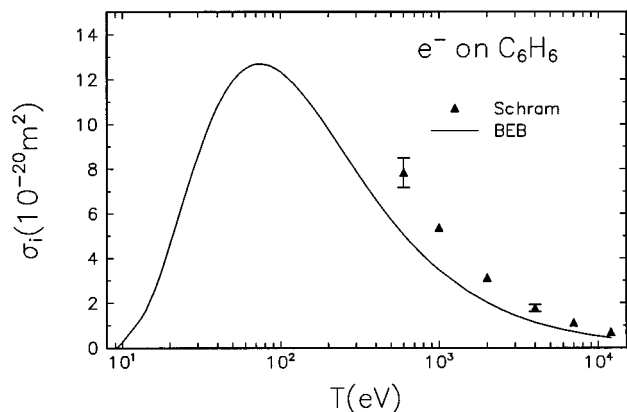


FIG. 15. Comparison of the BEB cross section to experiment for C_6H_6 . Solid curve, the BEB cross section; triangles, experimental data by Schram *et al.* (Ref. 37).

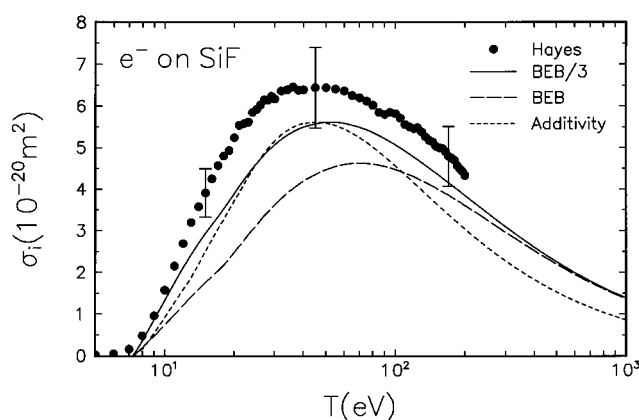


FIG. 16. Comparison of the BEB cross section to experiment for SiF. Solid curve, BEB cross section using modified values of U for the two outermost orbitals; long dashed curve, BEB cross section using unmodified U values; short dashed curve, additivity cross section based on the DM approach by Deutsch *et al.* (Ref. 6); circles, experimental data for SiF by Hayes *et al.* (Ref. 42).

from Si is transferred to F, and the effective ionization cross section comes from the remaining three valence electrons of Si. For SiF_2 , only two valence electrons of Si remains, and hence the total ionization cross section is smaller than that of SiF. The same logic explains why SiF_3 has smaller ionization cross section than the other two radicals.

So far, we have applied the BEB model to molecules made of light atoms that consisted of only K - and L -shell electrons. However, in our experience in applying the BEB model to Ar, Kr, and Xe, we found that the U values of M -shell and outer shell electrons had to be divided by their principal quantum numbers to obtain reliable ionization cross sections. Otherwise, BEB cross sections were too low at the peak. These outer shell electrons have radial nodes (in atomic orbitals) which make the U values very high. Note that the U values of the molecular orbitals identified with the M electrons of Si in Table III are more than five times the corresponding values of B . These large U values decrease the contributions from the valence electrons, which are usually the dominant ones.

We have applied the same remedy to the BEB cross sections for SiF, SiF_2 , and SiF_3 by reducing the U values of the valence molecular orbitals clearly identified with the $3s$ and/or $3p$ electrons of Si through the Mulliken population analysis. Such orbitals are identified in Table III, and their U values were divided by three as indicated in the table. As expected, the charge density of the two outermost orbitals of SiF and one valence orbital each in SiF_2 and SiF_3 are dominantly ($\geq 90\%$) from Si. For instance, we used $U(7\sigma) = 55.09/3 = 18.36$ eV, and $U(3\pi) = 34.39/3 = 11.46$ eV for SiF.

The BEB cross sections with these modified U values are compared to experimental data for SiF by Hayes *et al.*,⁴² SiF_2 by Shul *et al.*,⁴³ and for SiF_3 by Hayes *et al.*⁴⁴ in Figs. 16–18, respectively. The curves marked “BEB/3” represent BEB cross sections with the modified U values, while the

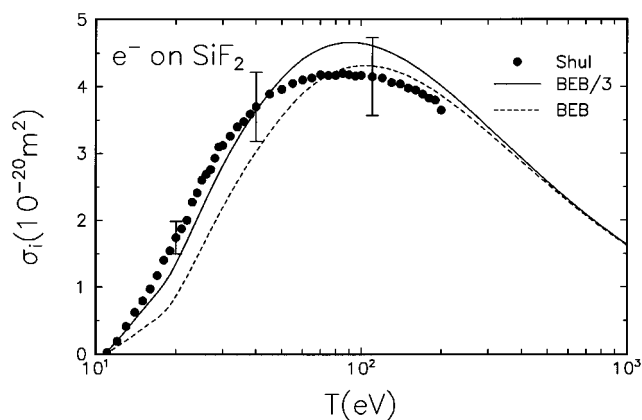


FIG. 17. Comparison of the BEB cross section to experiment for SiF_2 . Solid curve, BEB cross section using modified value of U for the outermost orbitals; dashed curve, BEB cross section using unmodified U value; circles, experimental data for SiF_2 by Shul *et al.* (Ref. 43).

curves marked “BEB” used the unmodified U values as we did for other molecules in this article.

Even with this modification, the BEB model grossly overestimates the cross section for SiF_3 in the peak region. A detailed analysis of the BEB cross section reveals that the contributions from the extra electrons in SiF_3 made its peak cross section comparable to that of SiF_2 contrary to the experiment. Since the UHF method tends to produce unreliable B values for outer valence electrons, SiF_3 may be a candidate for using data from a more sophisticated wave function. As is shown in Fig. 16, the DM approach⁶ also has difficulty as we do in reproducing the experimental data well.

On the other hand, we find in Fig. 19 that the BEB cross section for SF_6 is in reasonable agreement with the experiment by Rapp and Englander-Golden,¹⁵ probably because all valence electrons on S are strongly bound to F atoms, losing their atomic character according to the population analysis.

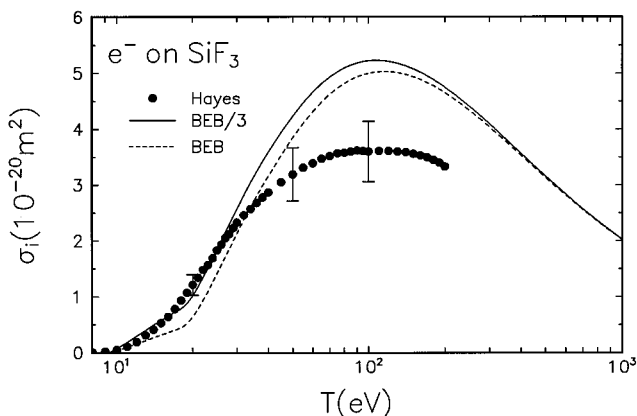


FIG. 18. Comparison of the BEB cross section to experiment for SiF_3 . Solid curve, BEB cross section using modified value of U for the outermost orbitals; dashed curve, BEB cross section using unmodified U value; circles, experimental data for SiF_3 by Hayes *et al.* (Ref. 44).

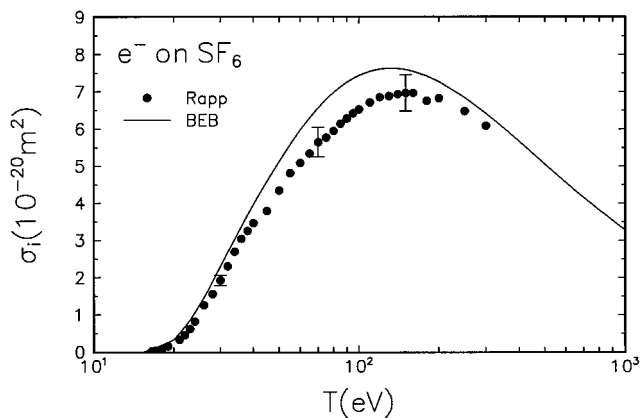


FIG. 19. Comparison of the BEB cross section to experiment for SF_6 . Solid curve, the BEB cross section; circles, experimental data by Rapp and Englander-Golden (Ref. 15).

Since no valence electron of SF_6 retained the M -shell characteristics of S, we used unmodified U values for all orbitals.

Ionization cross sections of fluorine compounds such as BF_x , CF_x , and SiF_x and similar chlorine compounds will serve as the “acid test” not only for the BEB model but also for any scheme that provides theoretical ionization cross sections.

IV. CONCLUSIONS

We have demonstrated that the BEB and BED cross sections provide reliable electron-impact total ionization cross sections for a large variety of molecules, except for SiF_3 , from ionization threshold to high incident energies, $T \sim 10$ keV. The BEB cross section requires only a minimal set of molecular constants for the initial state of the target molecule, which are readily available from public-domain molecular structure codes.

Moreover, the BEB equation consists of simple analytic expressions as functions of the incident energy for each molecular orbital that contributes to the ionization cross section, making the cross sections ideally suited for applications in modeling low-energy plasmas in plasma processing and fusion devices. When appropriate continuum oscillator strengths are available, the BED model provides better energy distribution of ejected electrons (singly differential cross sections) as well as total ionization cross sections. The BEB model uses far fewer constants than the additivity rules known as the DM approach. The latter also requires empirically fitted parameters, while our model has *no adjustable parameters*. Molecular orbital constants needed to construct BEB cross sections for 19 common molecules have been presented in Tables I–III.

The success of the BEB model on such a wide range of molecules is somewhat surprising, because our experience on atomic ionization cross sections clearly indicated that the BED model with appropriate continuum oscillator strengths was needed for good agreement with experiment. We speculate that the break-up of atomic orbitals to many molecular

orbitals in a molecule must act as a sort of “averaging” of atomic character and makes the BEB model adequate for most molecules.

Undoubtedly, a simple theory such as the BEB model will require further refinements to expand its application to a wider class of molecules, as we have already seen for fluorine compounds. Chlorine compounds are expected to have similar problems. Meanwhile, we are confident that the BEB model will reliably predict the ionization cross sections of hydrocarbons and other molecules made of light atoms, particularly closed-shell molecules.

BEB cross sections near the ionization threshold are sensitive to the lowest values of B and U used. To insure the proper behavior near the ionization threshold, experimental values of the lowest ionization potential, which are well known for many molecules and radicals,¹³ should be used as the lowest B . In some cases, cross sections near the threshold are also likely to be influenced by resonances and autoionization peaks, making it difficult for a simple theory such as the BEB or BED model to be universally effective.

For those who are interested in representing a known cross section by a simple analytic formula, Eq. (5) can be used—for the total ionization cross section, not orbital cross sections—by taking the lowest B to be the first ionization potential, as we did to insure proper ionization threshold, but treating U and N as fitting parameters. For instance, using a higher value of U for the outermost orbital in CH_4 and SF_6 (while keeping other constants to the values in Tables I–III) will reproduce the experimental cross sections by Rapp and Englander-Golden¹⁵ in Figs. 11 and 19 to a very high accuracy between the threshold and the peak without significantly altering the high- T part of the BEB cross section.

Work is in progress to extend the BEB model to other molecules of interest to air pollution and plasma chemistry modeling.

ACKNOWLEDGMENTS

We are grateful to the creators of the GAMESS code (see Ref. 12), without which we could not have carried out this work. We are indebted to Professor M. A. Ali for valuable advice on molecular wave functions, and to Dr. S. K. Srivastava, Professor T. M. Märk, and Professor R. F. Stebbings for providing tables of their experimental data. This work at NIST was supported in part by the Office of Fusion Energy of the U.S. Department of Energy, and at the University of Nebraska-Lincoln by the National Science Foundation Grant No. PHY-9119818.

¹I. Bray, *J. Phys. B* **28**, L247 (1995).

²N. F. Mott, *Proc. R. Soc. London Ser. A* **126**, 259 (1930).

³L. Vriens, in *Case Studies in Atomic Physics*, Vol. 1, edited by E. W. McDaniel and M. R. C. McDowell (North Holland, Amsterdam, 1969), p. 335.

⁴H. Bethe, *Ann. Phys.* **5**, 325 (1930).

⁵S. P. Khare and W. J. Meath, *J. Phys. B* **20**, 2101 (1987), and references therein.

⁶H. Deutsch, C. Cornelissen, L. Cespiva, V. Bonacic-Koutecky, D. Margreiter, and T. D. Märk, *Int. J. Mass Spectrom. Ion Processes* **129**, 43 (1993), and references therein.

⁷H. Deutsch, T. D. Märk, V. Tarnovsky, K. Becker, C. Cornelissen, L.

Cespiva, and V. Bonacic-Koutecky, *Int. J. Mass Spectrom. Ion Processes* **137**, 77 (1994), and references therein.

⁸S. M. Seltzer, in *Monte Carlo Transport of Electrons and Photons*, edited by T. M. Jenkins, W. R. Nelson, and A. Rindi (Plenum, New York, 1988), p. 81, and references therein.

⁹M. Gryzinski, *Phys. Rev.* **138**, A305 (1965); **138**, A322 (1965); **138**, A336 (1965).

¹⁰Y.-K. Kim and M. E. Rudd, *Phys. Rev. A* **50**, 3954 (1994).

¹¹W. Kołos and C. C. J. Roothaan, *Rev. Mod. Phys.* **32**, 205 (1960).

¹²We have used the version of GAMESS described by M. W. Schmidt, K. K. Baldrige, J. A. Boatz, S. T. Elbert, M. S. Gordon, J. H. Jensen, S. Koseki, N. Matsunaga, K. A. Nguyen, S. J. Su, T. L. Windus, M. Dupuis, and J. A. Montgomery, *J. Comput. Chem.* **14**, 1347 (1993).

¹³S. G. Lias, J. F. Liebman, R. D. Levin, and S. A. Kafafi, “NIST Positive Ion Energetics Database, Version 2.0,” Standard Reference Database 19A, National Institute of Standards and Technology, Oct. 1993.

¹⁴M. E. Rudd, Y.-K. Kim, D. H. Madison, and T. J. Gay, *Rev. Mod. Phys.* **64**, 441 (1992).

¹⁵D. Rapp and P. Englander-Golden, *J. Chem. Phys.* **43**, 1464 (1965).

¹⁶E. Krishnakumar and S. K. Srivastava, *J. Phys. B* **27**, L251 (1994). See also, E. Krishnakumar and S. K. Srivastava, *Abstracts, 16th Int. Conf. on the Physics of Electronic and Atomic Collisions*, edited by A. Dalgarno, R. S. Freund, M. S. Lubell, and T. B. Lucatorto (New York, 1989), p. 326.

¹⁷B. L. Schram, F. J. de Heer, M. J. van der Wiel, and J. Kistenmaker, *Physica* **31**, 94 (1965).

¹⁸B. L. Schram, H. R. Moustafa, J. Schutten, and F. J. de Heer, *Physica* **32**, 734 (1966).

¹⁹D. R. Schultz, L. Meng, and R. E. Olsen, *J. Phys. B* **25**, 4601 (1992).

²⁰D. Margreiter, H. Deutsch, M. Schmidt, and T. D. Märk, *Int. J. Mass Spectrom. Ion Processes* **100**, 157 (1990).

²¹E. Krishnakumar and S. K. Srivastava, *J. Phys. B* **23**, 1893 (1990).

²²H. C. Straub, P. Renault, B. G. Lindsay, K. A. Smith, and R. F. Stebbings (to be published).

²³E. Krishnakumar and S. K. Srivastava, *Int. J. Mass. Spectrom. Ion Processes* **113**, 1 (1992).

²⁴R. K. Asundi, J. D. Craggs, and M. V. Kurepa, *Proc. Phys. Soc. London* **82**, 967 (1963).

²⁵O. J. Orient and S. K. Srivastava, *J. Phys. B* **20**, 3923 (1987).

²⁶I. Iga, M. V. S. Rao, and S. K. Srivastava, *J. Geophys. Res.* (in press).

²⁷K. Kimura, S. Katsumata, Y. Achiba, T. Yamazaki, and S. Iwata, *Handbook of He I Photoelectron Spectra of Fundamental Organic Molecules* (Japan Scientific Societies, Tokyo, 1981), p. 29.

²⁸Y. B. Kim, K. Stephan, E. Märk, and T. D. Märk, *J. Chem. Phys.* **74**, 6771 (1981).

²⁹N. Lj. Durić, I. M. Čadež, and M. V. Kurepa, *Int. J. Mass. Spectrom. Ion Processes* **83**, R7 (1988).

³⁰M. A. Bolorizadeh and M. E. Rudd, *Phys. Rev. A* **33**, 882 (1985).

³¹J. Schutten, F. J. de Heer, H. R. Moustafa, A. J. H. Boerboom, and J. Kistenmaker, *J. Chem. Phys.* **44**, 3924 (1966).

³²M. V. S. Rao, I. Iga, and S. K. Srivastava, *J. Geophys. Res.* (in print).

³³N. Djurić, D. Belić, M. Kurepa, J. U. Mack, J. Rothleitner, and T. D. Märk, *Abstracts, 12th Int. Conf. on the Physics of Atomic and Electronic Collisions*, edited by S. Datz (Gatlinburg, 1981), p. 384.

³⁴M. V. S. Rao and S. K. Srivastava, *J. Phys. B* **25**, 2175 (1992).

³⁵H. Deutsch and M. Schmidt, *Beitr. Plasmaphys.* **24**, 475 (1984).

³⁶F. A. Baiocchi, R. C. Wetzel, and R. S. Freund, *Phys. Rev. Lett.* **53**, 771 (1984).

³⁷B. L. Schram, M. J. van der Wiel, F. J. de Heer, and H. R. Moustafa, *J. Chem. Phys.* **44**, 49 (1966).

³⁸N. Durić, I. Čadež, and M. Kurepa, *Int. J. Mass Spectrom. Ion Processes* **108**, R1 (1991).

³⁹H. Chatham, D. Hills, R. Robertson, and A. Gallagher, *J. Chem. Phys.* **81**, 1770 (1984).

⁴⁰V. Grill, G. Walder, P. Scheier, M. Krudel, and T. D. Märk, *Int. J. Mass Spectrom. Ion Processes* **129**, 31 (1993).

⁴¹V. Grill, G. Walder, D. Margreiter, T. Rauth, H. U. Poll, P. Scheier, and T. D. Märk, *Z. Phys. D* **25**, 217 (1993).

⁴²T. R. Hayes, R. C. Wetzel, F. A. Baiocchi, and R. S. Freund, *J. Chem. Phys.* **88**, 823 (1988).

⁴³R. J. Shul, T. R. Hayes, R. C. Wetzel, F. A. Baiocchi, and R. S. Freund, *J. Chem. Phys.* **89**, 4042 (1988).

⁴⁴T. R. Hayes, R. J. Shul, F. A. Baiocchi, R. C. Wetzel, and R. S. Freund, *J. Chem. Phys.* **89**, 4035 (1988).